Magnetic Circular Dichroism of Low-Spin d^6 Hexahalides of Iridium, Platinum, Palladium, and Rhodium

G. N. Henning,[1] P. A. Dobosh, A. J. McCaffery,[2] and P. N. Schatz

Contribution from the Department of Chemistry, University of Virginia, Charlottesville, Virginia 22901. *Received April 3, 1970*

Abstract: The magnetic circular dichroism (MCD) spectra of $IrCl_6^{3-}$, $PtCl_6^{2-}$, $PtBr_6^{2-}$, PtI_6^{2-}, $PdCl_6^{2-}$, $RhCl_6^{3-}$, and $RhBr_6^{3-}$ have been measured in solution over the region ~14,000–44,000 cm^{-1}. Attention is focused on a detailed interpretation of the ligand-to-metal charge-transfer spectra. The results in the chlorides can be understood neglecting ligand spin–orbit coupling (spin–orbit coupling of the d electrons plays no role), but its consideration is essential for the bromides and iodide. The more important features of the lower energy charge-transfer region can be understood by considering only states arising from the $t_{1u}(\pi)^6 \rightarrow t_{1u}(\pi)^5e_g$ excitation (with σ–π mixing), but a detailed interpretation requires extensive mixing with states arising from the $t_{2u}(\pi)^6 \rightarrow t_{2u}(\pi)^5e_g$ and $t_{1u}(\sigma)^6 \rightarrow t_{1u}(\sigma)^5e_g$ excitations.

In two recent papers[3,4] we have used magnetic circular dichroism (MCD) spectroscopy to assign charge-transfer transitions in several low-spin d^5 hexahalides. In particular, the relative order of the $t_{1u}(\pi)$ and $t_{2u}(\pi)$ ligand orbitals was established, the MCD results showing unambiguously that the $^2T_{2g}[t_{2g}^5] \rightarrow {}^2T_{1u}[t_{1u}(\pi)^5t_{2g}^6]$ transition is at lower energy than $^2T_{2g}[t_{2g}^5] \rightarrow {}^2T_{2u}[t_{2u}(\pi)^5t_{2g}^6]$. In this paper we shall be concerned chiefly with the charge-transfer transitions in low-spin d^6 octahedral hexahalides. We shall check the conventional assignments,[5] and by studying several of the ions as a function of ligand we shall be able to gain additional information about the spin–orbit splittings in the excited states. The theoretical analysis of MCD data has been discussed extensively in the papers referred to above[3,4] (and references therein), and a review article has also appeared recently.[6] Consequently, we shall not review the theoretical background of MCD spectroscopy here.

Experimental Section

MCD spectra were measured in the manner described previously,[7] and absorption spectra were recorded on a Cary 14. The MCD sign convention is the one now generally used with the Verdet constant of water in the visible region of the spectrum taken to be *negative*.

Crystalline samples of the following compounds were very kindly supplied by Dr. C. K. Jørgensen, the solvent used in recording the spectrum of each being shown in parentheses: $K_3IrCl_6 \cdot 6H_2O$ (6 *M* HCl), K_2PtBr_6 (0.01 *M* KBr), $Na_3RhCl_6 \cdot 12H_2O$ (8 *M* HCl), $Na_3RhBr_6 \cdot 6H_2O$ (6 *M* HBr). $H_2PtCl_6 \cdot 6H_2O$ (2 *M* HCl) was obtained from Fisher Scientific Co., and K_2PdCl_6 (2 *M* HCl + Cl_2) and K_2PtI_6 (0.2 *M* $HClO_4$ + KI) were obtained from Alfa Inorganics, Inc. In all cases, the MCD spectra were run several times in succession to check reproducibility and to confirm that no reaction was occurring in solution.

The MCD signal-to-noise ratio was quite favorable for these ions, and we estimate that our MCD data should be accurate to about ±15%.

Results and Discussion

Our experimental results are displayed in Figures 1–7. $[\theta]_M$ is the molar ellipticity (defined as in natural optical activity in degrees deciliter decimeter^{-1} mole^{-1}) per gauss in the direction of the light beam. ϵ is the molar extinction coefficient. We shall concentrate our discussion on the charge-transfer region of the spectra and shall discuss (in order of increasing ligand spin–orbit coupling) the chlorides and then the bromides and iodide.

$RhCl_6^{3-}$, $PdCl_6^{2-}$, $PtCl_6^{2-}$. The accessible charge-transfer region of the spectrum of these hexachlorides is quite simple, consisting of two strongly allowed bands separated by about 12,000 cm^{-1} in $PdCl_6^{2-}$ and $PtCl_6^{2-}$, with only the first band within range in $RhCl_6^{3-}$. (Only the d → d transitions are accessible in $IrCl_6^{3-}$, and we shall discuss their MCD very briefly at the end of the paper.) If we refer to the qualitative MO energy level diagram for an octahedral halide complex (Figure 8), we note that the lowest ligand-to-metal charge-transfer transitions will involve excitations into the $2e_g$ shell (d orbitals) since the t_{2g} shell is completely filled in a low-spin d^6 complex. (The lowest allowed transition from the $2t_{2g}$ shell—to $3t_{1u}$—is expected at very much higher energy since in the $d^{10}s^2$ systems[8] the $2a_{1g} \rightarrow 3t_{1u}$ transition itself occurs in the 30,000–40,000-cm^{-1} range.) The only possible allowed transitions involve t_{1u} or $t_{2u} \rightarrow 2e_g$ excitations. The states arising from the three possible excitations of this type are shown in Figure 9.

The key to understanding the spectra is the observation by Jørgensen[5] that ligand π to metal e_g transitions are expected to occur with very low intensities relative to ligand σ to metal e_g transitions. Thus the $t_{1u}(\pi) \rightarrow e_g$ transition occurs with appreciable intensity only because there is $t_{1u}(\pi)$–$t_{1u}(\sigma)$ mixing of the ligand orbitals, while the $t_{2u}(\pi) \rightarrow e_g$ transition is very weak because no such mixing is possible. We have checked these arguments in a semiquantitative way by comparing transition moment integrals computed using appropriate Slater orbitals for Pt and Cl. The $\sigma \rightarrow e_g$ transitions are found to be on the order of 100 times as intense as the $\pi \rightarrow e_g$. We therefore expect[5] the first strong band in the spectrum to be primarily $t_{1u}(\pi) \rightarrow e_g$ followed by the much stronger

(1) Based in part on a thesis submitted by G. N. Henning in partial fulfillment of the requirements for the Ph.D. degree, University of Virginia, 1968.

(2) Department of Chemistry, University of Sussex, Brighton, Sussex, England.

(3) G. N. Henning, A. J. McCaffery, P. N. Schatz, and P. J. Stephens, *J. Chem. Phys.*, **48**, 5656 (1968).

(4) A. J. McCaffery, P. N. Schatz, and T. E. Lester, *ibid.*, **50**, 379 (1969).

(5) C. K. Jørgensen, *Mol. Phys.*, **2**, 309 (1959).

(6) P. N. Schatz and A. J. McCaffery, *Quart. Rev., Chem. Soc.*, **23**, 552 (1969).

(7) P. N. Schatz, A. J. McCaffery, W. Suëtaka, G. N. Henning, A. B. Ritchie, and P. J. Stephens, *J. Chem. Phys.*, **45**, 722 (1966).

(8) C. K. Jørgensen, "Absorption Spectra and Chemical Bonding in Complexes," Pergamon Press, Oxford, 1962, Chapter 10.

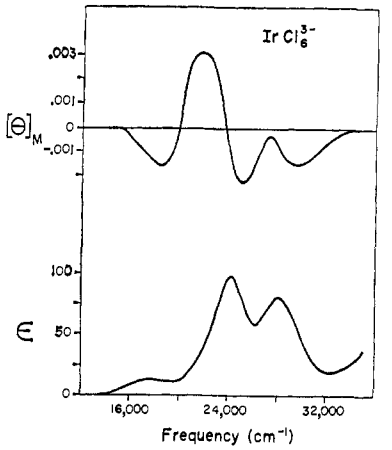

Figure 1. Absorption spectrum and MCD of $IrCl_6^{3-}$ in 6 *M* HCl. $[\theta]_M$ is the molar ellipticity (defined as in natural optical activity in degrees deciliter decimeter^{-1} mole^{-1}) per gauss in the direction of the light beam. ϵ is the molar extinction coefficient.

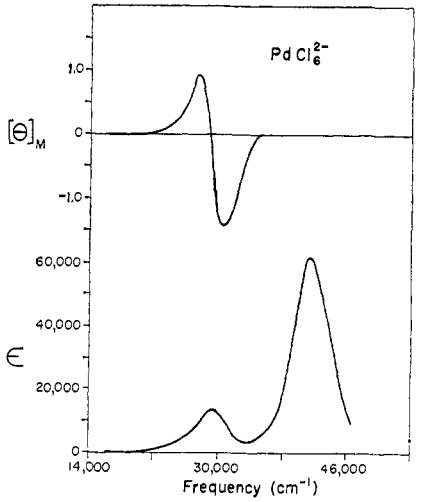

Figure 2. Absorption spectrum and MCD of $PdCl_6^{2-}$ in 2 *M* HCl + Cl_2. Symbols and units are as in Figure 1.

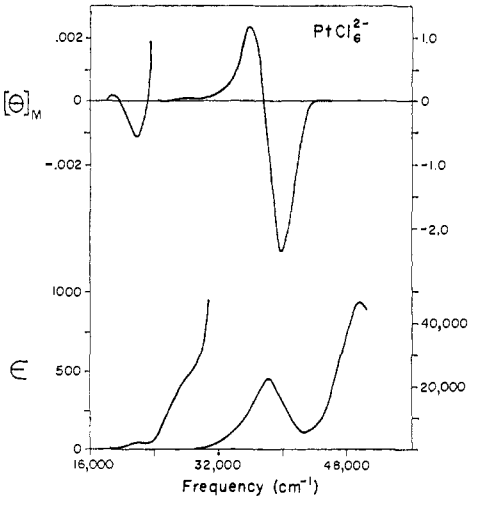

Figure 3. Absorption spectrum and MCD of $PtCl_6^{2-}$ in 2 *M* HCl. Symbols and units are as in Figure 1. Left-hand curves go with left scale and right-hand curves go with right scale.

$t_{1u}(\sigma) \rightarrow e_g$, the very weak $t_{2u}(\pi) \rightarrow e_g$ transition expected between these two not being observable. Assuming no spin–orbit coupling, the only allowed transitions are $^1A_{1g} \rightarrow {}^1T_{1u}$. If we also assume no

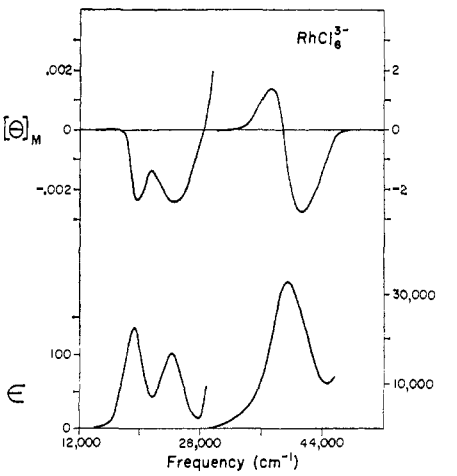

Figure 4. Absorption spectrum and MCD of $RhCl_6^{3-}$ in 8 *M* HCl. Symbols and units are as in Figure 1. Left-hand curves go with left scale and right-hand curves with right scale.

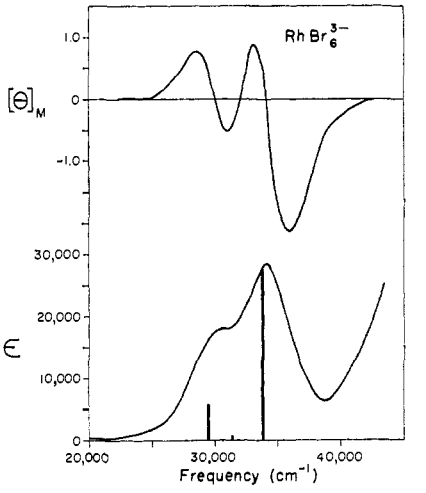

Figure 5. Absorption spectrum and MCD of $RhBr_6^{3-}$ in 6 *M* HBr. Symbols and units are as in Figure 1. The heights of the vertical bars are proportional to the calculated dipole strengths (*not* ϵ_{max} values).

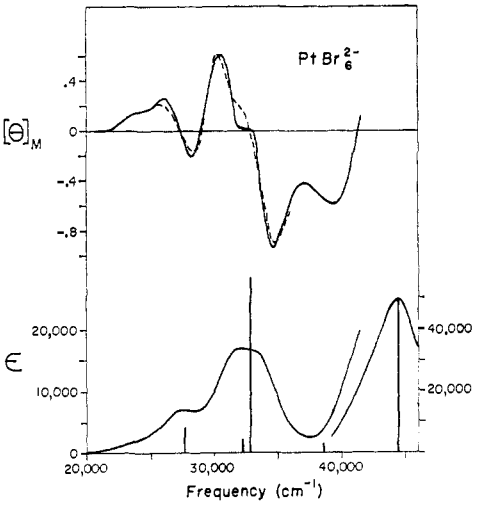

Figure 6. Absorption spectrum and MCD of $PtBr_6^{2-}$ in 0.01 *M* KBr. Symbols and units are as in Figure 1. The right-hand absorption curve goes with the right scale. The dashed curve shows a portion of the fit which gave rise to the experimental parameters in Table I. The heights of the vertical bars are proportional to the calculated dipole strengths (*not* ϵ_{max} values).

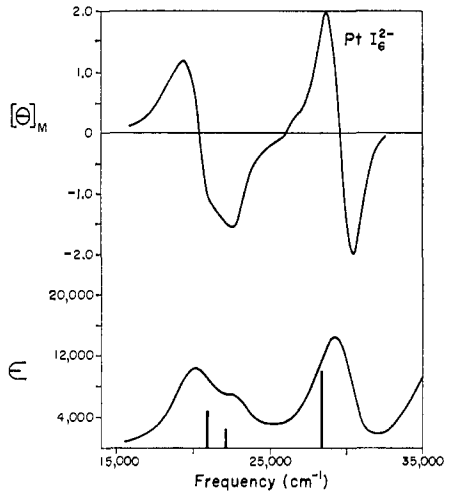

Figure 7. Absorption spectrum and MCD of PtI_6^{2-} in 0.2 M $HClO_4$ + KI. Symbols and units are as in Figure 1. The heights of the vertical bars are proportional to the calculated dipole strengths (*not* ϵ_{max} values).

$\sigma-\pi$ mixing, then the theoretically expected values of A/D are those shown in Figure 9. A/D is calculated using the conventions, notation, and method described previously,[7] with the result

$$A/D = \frac{-i}{\sqrt{2}}\langle {}^1T_{1u}||\mu||{}^1T_{1u}\rangle = \frac{-i}{2\sqrt{2}}\langle a||l||a\rangle \qquad (1)$$

with a $\equiv$ $t_{1u}(\pi)$, $t_{2u}(\pi)$, or $t_{1u}(\sigma)$, the reduced matrix element in each case being evaluated assuming pure ligand group orbitals and neglecting two-center terms. $\mu = -\beta(\mathbf{L} + 2\mathbf{S})$ is the magnetic moment operator and l is the one-electron orbital angular momentum operator. Thus on the basis of this simplest picture we expect the allowed bands to be unsplit with the lower energy one showing a negative A term and the higher one a zero A term. (Neglecting spin–orbit coupling, B terms for the ${}^1A_{1g} \rightarrow {}^1T_{1u}$ transition should arise only *via* mixing with states in other configurations and should be small.) In all three cases (Figures 2–4), the first band shows the expected negative A term. The neglect of spin–orbit coupling, supported by the lack of any observed splittings, seems well justified for the chlorides, since $\zeta_{Cl} = 587$ cm^{-1} [9] with observed band widths of the order of several thousand cm^{-1}. On the other hand, as discussed previously, the neglect of $\sigma-\pi$ mixing is not justified, and this will modify our simple theoretical predictions.

Using instead of $t_{1u}(\pi)$ and $t_{1u}(\sigma)$, the orbitals

$$t_{1u}' = at_{1u}(\pi) + bt_{1u}(\sigma) \qquad (2)$$

$$t_{1u}'' = -bt_{1u}(\pi) + at_{1u}(\sigma) \qquad (3)$$

with $a, b > 0$, we find for the reduced matrix elements of l

$$\langle t_{1u}'||l||t_{1u}'\rangle = \left\{a^2\left(\frac{i}{2}\right) + ab\sqrt{2}i\right\}\sqrt{2} \qquad (4)$$

$$\langle t_{1u}''||l||t_{1u}''\rangle = -\left\{b^2\left(\frac{i}{2}\right) - ab\sqrt{2}i\right\}\sqrt{2} \qquad (5)$$

The orbital t_{1u}' is of higher energy and is primarily $t_{1u}(\pi)$. The ratio of dipole strengths of the two bands in $PdCl_6^{2-}$ is ~3.2 to 1, and if, as a rough estimate, we choose a^2/b^2 to be in this ratio, we obtain $a \approx 0.87$ and $b \approx 0.49$. With these values, A/D for the lower and higher energy bands, respectively, becomes −0.49 and +0.24 as compared to −0.25 and 0.0 in the absence of $\sigma-\pi$ mixing. Thus the effect is to enhance the negative value observed for the lower energy band and to predict a nonzero (positive) value for the higher energy band. In accordance with this, we do observe that the experimental A/D values (Table I) for the lower energy bands of the chlorides are about −0.7. Unfortunately, we are not able to get reliable MCD results for the higher energy band in any of the chlorides. This band is out of range for $RhCl_6^{3-}$, and the onset of strong absorption by the HCl solvent prevents a reliable MCD measurement for $PtCl_6^{2-}$. In $PdCl_6^{2-}$, when the solution is made sufficiently dilute to obtain a usable optical density range, a reaction of some sort occurs preventing a reliable MCD measurement. We are thus unable to check the theoretical prediction of a clearly measurable positive A term for the higher energy band owing to the $\sigma-\pi$ mixing. We hope to be able to check this point at a later date by preparing a sample of $PdCl_6^{2-}$ doped into an appropriate host crystal.

(9) D. S. McClure, *J. Chem. Phys.*, 17, 905 (1949).

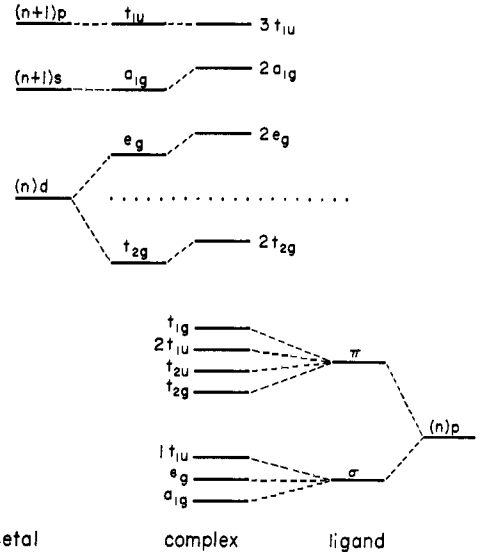

Figure 8. Schematic energy level diagram for an octahedral halide complex. In the d^6 case, all levels below the dotted line are filled. Allowed ligand-to-metal charge-transfer transitions to e_g can originate only from t_{1u} and t_{2u}.

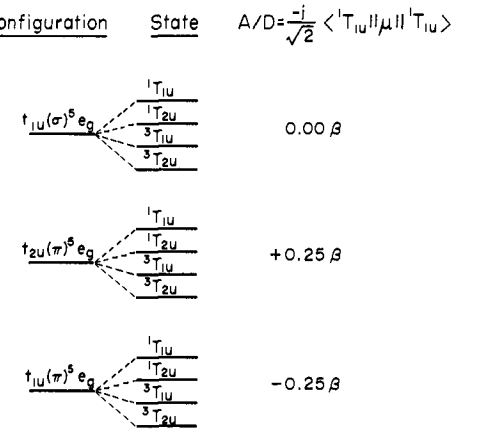

Figure 9. Lowest charge-transfer excited states for d^6 octahedral halides. A/D values shown are for the ${}^1A_{1g} \rightarrow {}^1T_{1u}$ transitions with no $\sigma-\pi$ mixing or spin–orbit coupling.

Table I.[a] Summary of Results and Assignments

Complex	Transition frequency, cm^{-1}	Assignment $^1A_{1g}\rightarrow$	$A/D^{b,c}$	$B/D^{b,c}$	$D^{b,c}$
$PdCl_6^{2-}$	29,400	$^1T_{1u}[t_{1u}'(\pi)^5e_g]$	−0.59 (−0.49) −0.68[d] (−0.49)	0.0001 (0)	26.1
	40,800	$^1T_{1u}[t_{1u}''(\sigma)^5e_g]$			83.2
$PtCl_6^{2-}$	(28,000)	$^3T_{1u}, ^3T_{2u}[t_{1u}'(\pi)^5e_g]$[e]			
	38,200	$^1T_{1u}[t_{1u}'(\pi)^5e_g]$	−0.58 (−0.49) −0.73 (−0.49)	−0.0002 (0)	34.0
	49,500	$^1T_{1u}[t_{1u}''(\sigma)^5e_g]$			66.8
$RhCl_6^{3-}$	39,400	$^1T_{1u}[t_{1u}'(\pi)^5e_g]$	−0.61 (−0.49) −0.66 (−0.49)	0.0001 (0)	52.5
$RhBr_6^{3-}$	(30,000)	$^3T_{1u}, ^3T_{2u}[t_{1u}'(\pi)^5e_g]$	−0.56 (−0.69)	0.0002 (0.0001)	17.2 (9.6)
	33,900	$^1T_{1u}[t_{1u}'(\pi)^5e_g]$	−0.80 (−0.55)	0.0000 (0.0000)	41.9 (41.9)
$PtBr_6^{2-}$	(23,000)	$^3T_{1u}, ^3T_{2u}[t_{1u}'(\pi)^5e_g]$[e]			
	27,700	$^3T_{1u}, ^3T_{2u}[t_{1u}'(\pi)^5e_g]$	−0.53 (−0.72)	0.0000 (0.0001)	11.3 (4.9)
	(31,900)	$^3T_{1u}, ^3T_{2u}[t_{2u}(\pi)^5e_g]$	+0.39 (0.48)	−0.0013 (−0.0060)	1.3[f] (1.9)
	(32,900)	$^1T_{1u}[t_{1u}'(\pi)^5e_g]$	−0.21 (−0.52)	0.0001 (0.0000)	22.2[f] (32.5)
	(40,500)	$^3T_{1u}, ^3T_{2u}[t_{1u}''(\sigma)^5e_g]$			
	44,500	$^1T_{1u}[t_{1u}''(\sigma)^5e_g]$			55.4 (55.4)
PtI_6^{2-}	20,000	$^3T_{1u}, ^3T_{2u}[t_{1u}'(\pi)^5e_g]$	−1.21 (−0.57)	−0.0002 (−0.0001)	15.6[f] (7.3)
	(22,500)	$^3T_{1u}, ^3T_{2u}[t_{2u}(\pi)^5e_g]$	0.34 (0.38)	0.0005 (0.0023)	8.1[f] (3.8)
	29,200	$^1T_{1u}[t_{1u}'(\pi)^5e_g]$	−0.51 (−0.57)	0.0002 (0.0000)	15.1 (15.1)

[a] Shoulders are in parentheses. [b] Theoretical value in parentheses; since theoretical D values are relative, they have been scaled for comparison with experimental D values. [c] Experimental value from gaussian fit except where noted. D is in square Debyes, A/D in Bohr magnetons, and B/D in Bohr magnetons/reciprocal centimeters. [d] Experimental A term determined by method of moments [see, for example, P. J. Stephens, *Chem. Phys. Lett.*, **2**, 241 (1968)]. [e] Tentative, see text. [f] Individual D values could not be obtained reliably by gaussian fitting, so total experimental dipole strength of the two transitions was divided in the ratio of the theoretically calculated D values (vertical bars in Figures 6 and 7).

$RhBr_6^{3-}$, $PtBr_6^{2-}$, PtI_6^{2-}. In the bromides and iodides, spin–orbit coupling is expected to be considerably more important (ζ_{Br} = 2457 cm^{-1} and ζ_I = 5069 cm^{-1}),[5] and the observed spectra are correspondingly more complex (Figures 5–7). Jørgensen has assigned these spectra in analogy with the hexachlorides so that the ~25,000–38,000-cm^{-1} region in $RhBr_6^{3-}$ and $PtBr_6^{2-}$ and the ~16,000–32,000-cm^{-1} region in PtI_6^{2-} are assigned to $t_{1u}(\pi) \rightarrow e_g$, the $t_{1u}(\sigma) \rightarrow e_g$ transition then corresponding to the more intense band at higher energy.

Let us now consider in some detail the consequences of spin–orbit coupling. It is convenient to work in the double group representation, and the various states in Figure 9 have the decompositions $^1T_{1u} = T_{1u}$, $^1T_{2u} = T_{2u}$, $^3T_{1u} = T_{1u} + T_{2u} + E_u + A_{1u}$, $^3T_{2u} = T_{1u} + T_{2u} + E_u + A_{2u}$. Allowed transitions are now $A_{1g} \rightarrow T_{1u}$ and thus each t_{1u} or $t_{2u} \rightarrow e_g$ excitation gives rise to three allowed transitions, where, however, the intensity is determined in each case by the amount of $^1T_{1u}$ contained in the T_{1u} states. The states $\psi_i(T_{1u})$ which result from spin–orbit coupling may be found by diagonalizing the Hamiltonian

$$H = H_{\text{electrostatic}} + H_{\text{spin-orbit}} \quad (6)$$

ψ_i will then be a linear combination of the nine T_{1u} components of the states of the three configurations. $H_{\text{spin-orbit}}$ is readily computed in terms of reduced matrix elements over ligand orbitals neglecting two center terms, but reliable values for the elements of the electrostatic Hamiltonian matrix are not easily obtained. The electrostatic Hamiltonian would be diagonal if the basis orbitals were self-consistent Hartree–Fock molecular orbitals (from Brillouin's theorem[10]). We shall proceed in a semiempirical way, setting off-diagnonal elements of the electrostatic Hamiltonian equal to zero and regarding the diagonal elements as parameters whose variation is to be examined in relation to the experimental data. We shall somewhat arbitrarily choose a = 0.87, b = 0.49 (eq 2 and 3) for all the chlorides, these values having been obtained from the $PdCl_6^{2-}$ spectrum as explained above, and a = 0.78, b = 0.63 for the bromides, obtained in the same way from the $PtBr_6^{2-}$ spectrum. Most of the final results are quite insensitive to the exact values used for these coefficients, and we shall point out in our later discussion that aspect for which this is not the case.

Rather than starting with a full treatment (nine T_{1u} states), we first use the simplest approximation and then examine the consequences of various refinements. We therefore start by considering only the $t_{1u}(\pi)^6 \rightarrow t_{1u}(\pi)^5e_g$ excitation including spin–orbit coupling, but $t_{1u}(\pi)$ now represents the σ–π-mixed t_{1u}' orbital. (Hereafter we shall designate the σ–π-mixed orbitals as $t_{1u}'(\pi)$ and $t_{1u}''(\sigma)$ in accordance with eq 2 and 3.) Calculations show that the σ–π mixing effectively reduces the spin–orbit interaction between the $t_{1u}(\pi)^5e_g$ configuration and the other two configurations, so we may anticipate a reasonably good description based on only this one configuration.

Reference to Figures 5 and 6 shows two distinct bands in the $t_{1u}'(\pi) \rightarrow e_g$ region with a clear indication of a third in $PtBr_6^{2-}$. PtI_6^{2-} (Figure 7) shows three bands clearly with the central band weakest.

Associated with the outer bands in all cases are negative A terms in MCD, while in PtI_6^{2-} a positive B and/or A term appears to be present for the middle band. The three by three Hamiltonian matrix is given by

(10) F. L. Pilar, "Elementary Quantum Chemistry," McGraw-Hill, New York, N. Y., 1968, p 364.

$$H_{\text{electrostatic}} = \begin{pmatrix} E(^1T_{1u}) & 0 & 0 \\ 0 & E(^3T_{1u}) & 0 \\ 0 & 0 & E(^3T_{2u}) \end{pmatrix} \quad (7)$$

$$H_{\text{spin-orbit}} = \begin{pmatrix} 0 & \frac{-1}{4\sqrt{2}} & \frac{\sqrt{6}}{8} \\ \frac{-1}{4\sqrt{2}} & \frac{-1}{8} & \frac{-\sqrt{3}}{8} \\ \frac{\sqrt{6}}{8} & \frac{-\sqrt{3}}{8} & \frac{1}{8} \end{pmatrix} \times K_{\pi\sigma}\zeta_{np} \quad (8)$$

where $K_{\pi\sigma}$ takes into account the effect of π–σ mixing. $K_{\pi\sigma} = 1$ for a pure $t_{1u}(\pi)$ orbital, 0 for $t_{1u}(\sigma)$, and ~2.0 for $t_{1u}'(\pi)$ with $a = 0.87$ and $b = 0.49$. It should be stressed that spin–orbit coupling in the charge-transfer excited states considered here depends only upon the *ligand* spin–orbit coupling parameter and thus is independent of the d-electron spin–orbit coupling. We now vary the energies of the electrostatic matrix and seek to explain the observed absorption and MCD spectra. If we write

$$\psi_i(T_{1u}) = a_i\phi(^1T_{1u}) + b_i\phi(^3T_{1u}) + c_i\phi(^3T_{2u}) \quad (9)$$

where $\phi(X)$ is the T_{1u} component of X, then it may be shown that

$$A_i/D_i = \frac{-i}{\sqrt{2}}\{a_i^2\langle\phi(^1T_{1u})||\mu||\phi(^1T_{1u})\rangle + b_i^2\langle\phi(^3T_{1u})||\mu||\phi(^3T_{1u})\rangle + c_i^2\langle\phi(^3T_{2u})||\mu||\phi(^3T_{2u})\rangle + 2b_ic_i\langle\phi(^3T_{1u})||\mu||\phi(^3T_{2u})\rangle\} \quad (10)$$

and

$$B_i/D_i = -i\sqrt{2}\sum_{k\neq i}\left\{\frac{1}{(E_k - E_i)}[a_ia_k\langle\phi(^1T_{1u})||\mu||\phi(^1T_{1u})\rangle + b_ib_k\langle\phi(^3T_{1u})||\mu||\phi(^3T_{1u})\rangle + c_ic_k\langle\phi(^3T_{2u})||\mu||\phi(^3T_{2u})\rangle + (b_ic_k + c_ib_k)\langle\phi(^3T_{1u})||\mu||\phi(^3T_{2u})\rangle]\frac{a_k}{a_i}\right\} \quad (11)$$

where the sum (over k) runs over the other two T_{1u} states of the configuration. It should also be noted that

$$D_i(A_{1g} \rightarrow \psi_i) = |a_i|^2 D(^1A_{1g} \rightarrow {}^1T_{1u}) \quad (12)$$

so that $|a_i|^2$ is a direct measure of the intensity of the band. We will use a simplified notation to denote transitions; *e.g.*, $A_{1g} \rightarrow \psi_i$ will be written as $^1A_{1g} \rightarrow {}^1T_{1u}$, where the excited state ($^1T_{1u}$ in the example) denotes the principal component(s) of the state ψ_i. When necessary, the excited-state configuration will be included in brackets with the configuration [a^5e_g] abbreviated as [a]. The triplet states are expected to be lower in energy than the singlet states, and eigenvectors were calculated for a range of energies using this assumption. Characteristic of the calculations is the fact that two intense bands are predicted, the higher energy one being more intense and predominantly $^1A_{1g} \rightarrow {}^1T_{1u}$ with the other predominantly $^1A_{1g} \rightarrow {}^3T_{1u}$, $^3T_{2u}$. The calculated intensity ratio of the two bands varied from 1:1 to 3:1. At lower energy than either of these bands, a very weak band ($|a_i|^2 < 0.02$) is predicted. This band is found to disappear entirely when $^3T_{1u}$ and $^3T_{2u}$ are degenerate. Each of the strong bands possesses a negative A/D term (eq 10) in agreement with experiment, while B/D terms (eq 11) are negligible. (Theoretical and experimental parameters are summarized in Table I.) The very weak band, which is also a $^1A_{1g} \rightarrow {}^3T_{1u}$, $^3T_{2u}[t_{1u}'(\pi)]$ transition, has a positive A/D with a negligible B term. The low intensity of the weak band and the fact that it should appear at a lower energy than the other two makes the central shoulder at ~22,500 cm^{-1} in the PtI_6^{2-} spectrum an unlikely candidate for this assignment. The same remark applies for the central shoulder in the $PtBr_6^{2-}$ spectrum (~32,000 cm^{-1}). In fact, in both $PtBr_6^{2-}$ and PtI_6^{2-} there is a weak shoulder at lower energy (~25,000 cm^{-1} in $PtBr_6^{2-}$ and ~17,000 cm^{-1} in PtI_6^{2-}) and a corresponding slight inflection in the MCD. This feature may well correspond to the predicted weak band.

Thus while the simplest treatment accounts for two of the observed bands, it is clear that a consideration of other configurations will be necessary to account for the third, central absorption band. The T_{1u} states of $t_{2u}(\pi)^5e_g$ and $t_{1u}''(\sigma)^5e_g$ were added to the calculation so that a 9 × 9 Hamiltonian was diagonalized. An extensive, though not exhaustive, variation of the electrostatic energies was carried out to find parameters which best fit the experimental results. To reduce the number of calculations to a reasonable level, the $^3T_{1u}$ and $^3T_{2u}$ states of each configuration were usually assumed to be degenerate. (Calculations without this restriction changed the results negligibly, adding only numerous, extremely weak transitions.) In addition, all singlet–triplet separations were assumed equal. That the separation between the $^1T_{1u}$ states of $t_{1u}'(\pi)^5e_g$ and $t_{1u}''(\sigma)^5e_g$ is at least 11,000 cm^{-1} in all three ions is clear from the spectra, but the location of the $t_{2u}(\pi)^5e_g$ states had to be found by varying their energies and comparing the calculated results with the spectra. As before, the $t_{1u}{}^5e_g$ configurations each gave rise to an intense $^1A_{1g} \rightarrow {}^1T_{1u}$ transition and a lesser $^1A_{1g} \rightarrow {}^3T_{1u}$, $^3T_{2u}$ transition. The $t_{2u}(\pi)^5e_g$ configuration, however, contributes only *one* band of appreciable intensity, namely $^1A_{1g} \rightarrow {}^3T_{1u}$, $^3T_{2u}[t_{2u}]$. This transition gains its intensity by mixing with the $^1T_{1u}$ components of the $t_{1u}'(\pi)^5e_g$ and $t_{1u}''(\sigma)^5e_g$ configurations. The contribution of $^1T_{1u}[t_{1u}''(\sigma)]$ to this band is relatively insensitive to the location of the $^3T_{1u}[t_{2u}]$ and $^3T_{2u}[t_{2u}]$ states and is sufficient to give the band an intensity as high as $^1/_{10}$th that of the $^1A_{1g} \rightarrow {}^1T_{1u}[t_{1u}'(\pi)]$ band. The $^1T_{1u}[t_{1u}'(\pi)]$ contribution to this band is noticeable, however, only when the $t_{2u}{}^5e_g$ triplet states are below $^1T_{1u}[t_{1u}'(\pi)]$ in energy and becomes very important when the $^3T_{1u}[t_{2u}]$ states are nearly degenerate with the $^3T_{1u}[t_{1u}'(\pi)]$ states. The intensity of this center band is also sensitive to the σ–π mixing coefficients a and b, for the relative phases of the $^1T_{1u}[t_{1u}]$ eigenvector coefficients depend upon the a and b parameters and the location of the central band. For the $PtBr_6^{2-}$ values of a and b, the contributions reinforce when the central band is at high energies (near $^1A_{1g} \rightarrow {}^1T_{1u}[t_{1u}'(\pi)]$) and tend to cancel when the band is at lower energies (near $^1A_{1g} \rightarrow {}^3T_{1u}$, $^3T_{2u}[t_{1u}'(\pi)]$). The situation is exactly the opposite for the $PdCl_6^{2-}$ a and b values. The other two T_{1u} states arising from $t_{2u}(\pi)^5e_g$ have only negligible $^1T_{1u}[t_{1u}'(\pi)]$ and $^1T_{1u}[t_{1u}''(\sigma)]$ components so a maximum of five strong bands is expected, as indeed is observed clearly in PtI_6^{2-}. (Figure 7

shows only the first three bands, but there are two much stronger bands[5]—at 39,800 and 43,500 cm^{-1}—which clearly should be associated with $t_{1u}''(\sigma) \rightarrow e_g$ transitions.) With these considerations in mind, the interpretation of the spectra is relatively straightforward. In Figures 5–7, the heights of the vertical bars are proportional to the dipole strengths calculated using the best set of energy parameters for each ion. (Note that the D values, and hence the height of the vertical bars, are not quantitatively related to ϵ_{max} values.) ζ_{np} was set at 2500 cm^{-1} for Br and 5000 cm^{-1} for I.

In the spectrum of $RhBr_6^{3-}$, only the $^1A_{1g} \rightarrow {}^1T_{1g}[t_{1u}'(\pi)]$ and $^1A_{1g} \rightarrow {}^3T_{1u}, {}^3T_{2u}[t_{1u}'(\pi)]$ bands are visible below the $^1A_{1g} \rightarrow {}^1T_{1u}[t_{1u}''(\sigma)]$ band, and the calculated and observed A/D values (Table I) are in quite reasonable agreement. There is no evidence of a $t_{2u}(\pi) \rightarrow e_g$ transition, and our calculation (Figure 5) indicates that this band will not be seen because of its very low intensity. In $PtBr_6^{2-}$, a third band is clearly visible in the $t_{1u}'(\pi) \rightarrow e_g$ region as a shoulder on the $^1A_{1g} \rightarrow {}^1T_{1u}[t_{1u}'(\pi)]$ band. It seems most likely from our calculations that the large negative A term is associated with the high energy shoulder and corresponds to $^1A_{1g} \rightarrow {}^1T_{1u}[t_{1u}'(\pi)]$, while the lower energy shoulder is the less intense $^1A_{1g} \rightarrow {}^3T_{1u}, {}^3T_{2u}[t_{2u}(\pi)]$ transition. The $t_{1u}'(\pi) \rightarrow e_g$ bands are predicted to have sizable negative A terms (and nearly zero B terms) which are relatively insensitive to variations of the energy parameters. Though the $^1T_{1u}[t_{1u}]$ components of the $t_{2u} \rightarrow e_g$ transition reinforce each other, ϵ_{max} for this band is still predicted to be only ~2000. We believe that the flattening observed at the center of the large negative A term (~32,500 cm^{-1}) is due to the positive A term associated with the $^1A_{1g} \rightarrow {}^3T_{1u}, {}^3T_{2u}[t_{2u}(\pi)]$ shoulder. The least-squares fit of the MCD obtained in the standard way[7] is shown by the dashed line (Figure 6), and there is a qualitative mimicking of this feature which, in fact, could be improved by further moderate adjustments of the parameters. The agreement between the calculated and observed A/D values (Table I) for $PtBr_6^{2-}$ is not unreasonable, especially in view of the somewhat arbitrary division of dipole strength between the two bands in the 32,000-cm^{-1} region. The MCD of $PtBr_6^{2-}$ also seems to show the beginning of a positive A term, starting at 35,000 cm^{-1}, which is associated with a very slight shoulder in the $^1A_{1g} \rightarrow {}^1T_{1u}[t_{1u}''(\sigma)]$ band at 40,500 cm^{-1}. Calculated A/D values are positive for this shoulder ($^1A_{1g} \rightarrow {}^3T_{1u}, {}^3T_{2u}[t_{1u}''(\sigma)]$) if the energy of $^3T_{1u}[t_{1u}''(\sigma)]$ is lower than that of $^3T_{2u}[t_{1u}''(\sigma)]$, and negative otherwise, and Jørgensen[5] has stated that the former case is more likely, in agreement with our observation.

In the spectrum of PtI_6^{2-}, the $^1A_{1g} \rightarrow {}^3T_{1u}, {}^3T_{2u}[t_{2u}]$ band (the center shoulder) has moved to a lower energy with respect to the $t_{1u}'(\pi)^5e_g$ states and appears to show a positive A and/or B term in the MCD. Using, as previously, the relative areas of the $t_{1u}'(\pi)$ and $t_{1u}''(\sigma)$ bands as a measure of $\sigma-\pi$ mixing, one finds a and b values (eq 2 and 3) of about the same magnitude as for $PdCl_6^{2-}$; *i.e.*, the mixing in the iodide is considerably lower than in the bromide. This is confirmed by the observed intensity of the center shoulder which one finds is much too low if the $PtBr_6^{2-}$ a and b values are used. Again the calculated A terms for the outer bands (~20,000 and ~29,500 cm^{-1}) are negative as observed experimentally, and positive A and B terms are predicted for the center shoulder, also in agreement with experiment (Table I). The sign of the calculated A term, particularly, seems quite insensitive to reasonable variations of the parameters and fits nicely with the observed MCD associated with the central shoulder. The best overall results for the PtI_6^{2-} data are obtained if the $t_{2u}{}^5e_g$ states are almost degenerate with those of $t_{1u}'(\pi)^5e_g$, indicating that the $t_{2u}(\pi)$ molecular orbitals are only slightly lower in energy than the $t_{1u}(\pi)$ in this complex. Unfortunately, we were not able to make reliable MCD measurements in the $t_{1u}''(\sigma) \rightarrow e_g$ region. We assign the bands reported by Jørgensen[5] at 39,800 and 43,500 cm^{-1} as $^1A_{1g} \rightarrow {}^3T_{1u}, {}^3T_{2u}[t_{1u}''(\sigma)]$ and $^1A_{1g} \rightarrow {}^1T_{1u}[t_{1u}''(\sigma)]$, respectively.

d–d Spectra. Jørgensen[11] has measured the crystal-field spectra of $RhCl_6^{3-}$ and $IrCl_6^{3-}$, and our measurements reproduce his results. All the bands arise from the $t_{2g}{}^6 \rightarrow t_{2g}{}^5e_g$ transition. The strong bands (ϵ ~100) at 19,300 and 24,200 cm^{-1} in $RhCl_6^{3-}$ and at 24,400 and 28,200 cm^{-1} in $IrCl_6^{3-}$ are assigned to $^1A_{1g} \rightarrow {}^1T_{1g}$ and $^1A_{1g} \rightarrow {}^1T_{2g}$, respectively, on the basis of crystal-field calculations. The weak bands (ϵ ~10) visible in the $IrCl_6^{3-}$ spectrum at 15,000–19,000 cm^{-1} are believed to be $^1A_{1g} \rightarrow {}^3T_{1g}$ and $^1A_{1g} \rightarrow {}^3T_{2g}$. According to Stephens,[12] the sign of the MCD of each vibronic transition will depend upon whether the transition arises *via* a t_{1u} or t_{2u} vibration. The MCD at room temperature is thus difficult to interpret and any conclusions from the MCD must await low temperature studies which may resolve the vibronic fine structure.

Conclusions

The low-energy charge-transfer region of the chlorides can be understood without considering spin–orbit coupling. The observed intensities require $\sigma-\pi$ mixing which in fact also improves the agreement between the calculated and observed MCD A terms. This same spectral region is much more complicated in the bromides and iodide and clearly requires a detailed consideration of spin–orbit coupling. The two large negative A terms observed can be accounted for by considering spin–orbit coupling only within the $t_{1u}(\pi)^5e_g$ excited configuration, but an explanation of the observed features of the central band in this region (in $PtBr_6^{2-}$ and PtI_6^{2-}) requires extensive mixing with states from the higher energy $t_{2u}(\pi)^5e_g$ and $t_{1u}(\sigma)^5e_g$ configurations. The appearance of two strong bands in the higher energy $t_{1u}(\sigma)^5e_g$ region of the spectrum, indicated in $PtBr_6^{2-}$ and observed more clearly in PtI_6^{2-}, is a direct consequence of spin–orbit coupling in the $t_{1u}(\sigma)^5e_g$ excited configuration.

Acknowledgments. We wish to thank Dr. D. D. Shillady for the use of his extended Hückel program for checking the relative values predicted for π and $\sigma \rightarrow e_g$ ligand-to-metal transition moments. We greatly appreciate the help of Dr. J. R. Dickinson with a number of experimental problems. We are very much indebted to Dr. C. K. Jørgensen for supplying us with a number of chemical samples. This work was supported by the National Science Foundation.

(11) C. K. Jørgensen, *Acta Chem. Scand.*, 10, 500 (1956).
(12) P. J. Stephens, *J. Chem. Phys.*, 44, 4060 (1966).